Final Project Report: Stars, from Newton to Einstein

Kübra Büber

Koç University • Physics Department

Abstract

This report delves into the theoretical and numerical aspects of stellar structure, focusing on two pivotal equations in astrophysics: the Lane–Emden equation for polytropic stars and the Tolman-Oppenheimer-Volkoff (TOV) equation for neutron stars. The study begins with the derivation and solution of the Lane–Emden equation, illustrating its role in determining mass-radius relationships for stars and white dwarfs. Observational data from the Montreal White Dwarf Database is used to validate theoretical models. In the second part, the TOV equation is solved for neutron stars under a polytropic equation of state. Key properties, such as mass, radius, and fractional binding energy, are computed. The results demonstrate the importance of both Newtonian and relativistic frameworks in understanding stellar evolution and provide insights into the maximum stable configurations of neutron stars.

Introduction

Understanding the internal structure of stars is a cornerstone of astrophysics, offering insights into their life cycles, stability, and ultimate fate. The study of stellar structure is rooted in two fundamental principles: hydrostatic equilibrium and the equation of state (EOS). Together, these principles govern the intricate balance between gravitational collapse and pressure forces, shaping the evolution of stars from their birth to end stages, such as white dwarfs and neutron stars.

This report explores the Lane–Emden equation, derived under the assumption of a polytropic EOS, to model the internal structure of stars in Newtonian gravity. The solutions provide valuable insights into the mass-radius relationships of stars and white dwarfs. Observational data is analyzed to bridge the gap between theory and observation, validating the Lane–Emden framework.

For compact objects like neutron stars, where densities and gravitational fields are extreme, Newtonian mechanics is insufficient. The Tolman-Oppenheimer-Volkoff (TOV) equation, derived from general relativity, becomes essential to model these objects accurately. This report investigates the TOV equation with a polytropic EOS, exploring the mass-radius relationship, fractional binding energy, and stability of neutron stars.

By combining analytical derivations, numerical simulations, and observational data, this study provides a comprehensive understanding of stellar structure, highlighting the transition from Newtonian to relativistic regimes.

Newton

Part A: Lane-Emden Equation and Its Properties

The study of stellar structure is fundamental in astrophysics, providing insights into the internal composition and behavior of stars. A key concept in this field is **hydrostatic equilibrium**, which describes the balance between the inward gravitational force and the outward pressure gradient within a star. When coupled with an appropriate **equation of state** (EOS) that relates pressure to density, these principles allow us to model the internal structure of stars. A particularly elegant formulation arises under the assumption of a *polytropic* EOS, leading to the renowned **Lane–Emden equation**.

Governing Equations of Stellar Structure

The two principal ODEs for a spherically symmetric star in Newtonian gravity can be written as:

- *Mass continuity:*

$$\frac{dm(r)}{dr} = 4\pi r^2 \rho(r), \tag{1}$$

- *Hydrostatic equilibrium:*

$$\frac{dP(r)}{dr} = -\frac{G\, m(r)\, \rho(r)}{r^2}, \tag{2}$$

where $m(r)$ is the mass enclosed within radius r, $\rho(r)$ is the density, $P(r)$ the pressure, and G the gravitational constant.

These two equations contain three unknowns: $m(r)$, $\rho(r)$, and $P(r)$. To close the system, we need an equation of state $P(\rho)$.

Polytropic Equation of State (EOS)

A frequently used EOS in stellar astrophysics is the *polytropic* equation of state:

$$P = K\rho^{\gamma} = K\rho^{1+\frac{1}{n}}, \tag{3}$$

where $\gamma = 1 + \frac{1}{n}$. The constant K is sometimes called the polytropic constant, and n the polytropic index.

From Hydrostatic Equilibrium to Lane–Emden

Starting with Eqs. (1) and (2), we have

$$\frac{dm}{dr} \;=\; 4\pi r^2 \rho, \quad \frac{dP}{dr} \;=\; -\frac{G\,m(r)\,\rho}{r^2}.$$

Rearrange the second equation,

$$\frac{r^2}{\rho}\,\frac{dP}{dr} \;=\; -G\,m(r).$$

Next, differentiate the left-hand side w.r.t. r:

$$\frac{d}{dr}\!\left(r^2\,\frac{1}{\rho}\,\frac{dP}{dr}\right) \;=\; -G\,\frac{dm}{dr}.$$

Using $\frac{dm}{dr} = 4\pi r^2 \rho$,

$$\frac{d}{dr}\!\left(r^2\,\frac{1}{\rho}\,\frac{dP}{dr}\right) = -4\pi\,G\,r^2\,\rho.$$

Divide both sides by r^2:

$$\frac{1}{r^2}\,\frac{d}{dr}\!\left(r^2\,\frac{1}{\rho}\,\frac{dP}{dr}\right) \;=\; -4\pi\,G\,\rho. \tag{4}$$

This single differential equation, however, still involves both P and ρ. We now assume the polytropic relation $P = K\,\rho^{\gamma}$ to link P and ρ.

Define

$$\rho(r) \;=\; \rho_c\,\theta^n(r), \tag{5}$$

where ρ_c is the central density and $\theta(r)$ is a dimensionless function (with $\theta(0) = 1$). For the pressure, using the polytrope,

$$P(r) \;=\; K\,\rho^{\gamma}(r) \;=\; K\,\rho_c^{\gamma}\,\theta^{n+1}(r). \tag{6}$$

A characteristic length scale α is defined via:

$$\alpha^2 \;=\; \frac{(n+1)\,K\,\rho_c^{\frac{1}{n}-1}}{4\pi\,G} \quad\Longleftrightarrow\quad \alpha \;=\; \left(\frac{(n+1)\,K\,\rho_c^{\frac{1}{n}-1}}{4\pi\,G}\right)^{\frac{1}{2}}. \tag{7}$$

The dimensionless radius $\xi = \frac{r}{\alpha}$ is introduced.

Substitute (5) and (6) into (4). After some algebra and cancellations, one arrives at the classic **Lane–Emden equation** for $\theta(\xi)$:

$$\frac{1}{\xi^2}\,\frac{d}{d\xi}\!\left(\xi^2\,\frac{d\theta}{d\xi}\right) \;+\; \theta^n \;=\; 0. \tag{8}$$

Series Solution Near the Center

A physically acceptable solution must remain finite at $\xi = 0$. One seeks a power-series expansion of the form

$$\theta(\xi) \;=\; 1 \;+\; a_2\,\xi^2 \;+\; a_4\,\xi^4 \;+\; \dots \tag{9}$$

By plugging this into the Lane–Emden equation (8) and matching powers of ξ, one finds

$$a_2 \;=\; -\tfrac{1}{6}, \quad a_4 \;=\; \tfrac{n}{120}, \quad \dots$$

Thus,

$$\theta(\xi) \;=\; 1 \;-\; \frac{1}{6}\,\xi^2 \;+\; \frac{n}{120}\,\xi^4 \;+\; \dots \tag{10}$$

This shows how $\theta(\xi)$ remains *regular* (finite and smooth) at the center $\xi = 0$.

Analytical Solution for $n = 1$

When $n = 1$, we have $\gamma = 2$, and Eq. (8) becomes

$$\frac{1}{\xi^2}\,\frac{d}{d\xi}\big(\xi^2\,\tfrac{d\theta}{d\xi}\big) \;+\; \theta \;=\; 0. \tag{11}$$

This is essentially a spherical Bessel equation. The general solution is

$$\theta(\xi) \;=\; A\,\frac{\sin(\xi)}{\xi} \;+\; B\,\frac{\cos(\xi)}{\xi}.$$

Regularity at $\xi = 0$ forces $B = 0$. We also require $\theta(0) = 1$, which is satisfied by $\sin(\xi)/\xi$. Hence the well-known solution:

$$\theta(\xi) \;=\; \frac{\sin(\xi)}{\xi}. \tag{12}$$

The zero of $\sin(\xi)$ at $\xi = \pi$ gives a *finite* boundary (since $\theta(\pi) = 0$ implies $\rho(\pi) = 0$), thus bounding the star's radius in this model.

Mass Integral and Dimensionless Form

The total mass M is found by integrating the density over the entire stellar volume:

$$M \;=\; \int_0^R 4\pi\,r^2\,\rho(r)\,dr. \tag{13}$$

Using $r = \alpha\,\xi$, $\rho(r) = \rho_c\,\theta^n(\xi)$, and the fact that the star's surface occurs at $\xi = \xi_n$ (where $\theta(\xi_n) = 0$), we have

$$M \;=\; 4\pi\,\alpha^3\,\rho_c \int_0^{\xi_n} \xi^2\,\theta^n(\xi)\,d\xi. \tag{14}$$

From the Lane–Emden equation, one can show

$$\xi^2\,\theta^n \;=\; -\frac{d}{d\xi}\!\left(\xi^2\,\frac{d\theta}{d\xi}\right),$$

hence

$$\int_0^{\xi_n} \xi^2\,\theta^n\,d\xi \;=\; -\left[\xi^2\,\frac{d\theta}{d\xi}\right]_0^{\xi_n} \;=\; -\xi_n^2\left(\tfrac{d\theta}{d\xi}\right)_{\xi_n},$$

the lower endpoint vanishing because θ is regular at $\xi = 0$. Therefore,

$$M \;=\; -4\pi\,\alpha^3\,\rho_c\,\xi_n^2\left(\frac{d\theta}{d\xi}\right)_{\xi_n}. \tag{15}$$

Recalling $R = \alpha\,\xi_n$, or $\alpha = R/\xi_n$, one arrives at

$$M \;=\; 4\pi\,\rho_c\,R^3\!\left(-\frac{\theta'(\xi_n)}{\xi_n}\right). \tag{16}$$

This furnishes the total mass explicitly in terms of the central density ρ_c, the radius R, and the Lane–Emden solution $\theta(\xi)$.

Mass–Radius Relation for Polytropes

If a family of stars shares the same polytropic index n (and same constant K), then one can eliminate ρ_c to get a relation $M(R)$. From

$$\alpha^2 = \frac{(n+1)\,K\,\rho_c^{\frac{1}{n}-1}}{4\pi\,G},$$

one can solve for ρ_c in terms of α (and hence R). Substituting back, one obtains the well-known homology relation:

$$M \propto R^{\frac{3-n}{1-n}} \implies M = A\,R^{\frac{3-n}{1-n}}, \tag{17}$$

for some constant A that depends on n, K, and the specific Lane–Emden solution $\theta(\xi)$. In particular,

$$A = -4\pi \left(\frac{4\pi G}{K(n+1)}\right)^{\frac{n}{1-n}} \xi_s^{-\frac{1+n}{1-n}}\,\theta'(\xi_s) \tag{18}$$

showing explicitly how B depends on the chosen EOS.

Part B: White Dwarf Mass-Radius Relationship Data Observation

The observational data was obtained from the Montreal White Dwarf Database (MWDD), focusing on relatively cold white dwarfs to minimize temperature-related effects on the EOS. The dataset includes two primary quantities for each white dwarf:

- **Mass (M)**: Measured in solar masses ($M_\odot$).
- **Surface Gravity** ($\log(g)$): Given as the base-10 logarithm of surface gravity in CGS units (cm/s^2).

The surface gravity $\log(g)$ was converted to physical units using:

$$g = 10^{\log(g)}\ \text{cm/s}^2$$

Using Newtonian gravity, the radius R of each white dwarf was calculated from:

$$g = \frac{GM}{R^2} \implies R = \sqrt{\frac{GM}{g}}$$

where:

- $G = 6.6743 \times 10^{-11}\ \text{m}^3\,\text{kg}^{-1}\,\text{s}^{-2}$ (gravitational constant in SI units).
- M is the mass in kilograms ($M_\odot = 1.989 \times 10^{30}$ g).

The calculated radii were then converted to Earth radii ($R_\oplus = 6.371 \times 10^6$ m) for easier interpretation.

Two plots were generated to visualize the mass-radius relationship as seen in Figure 1 and Figure 2:

1. **Linear Scale Scatter Plot**: Displays mass versus radius on a linear scale.
2. **Log-Log Scale Scatter Plot**: Provides a logarithmic perspective to identify scaling laws.

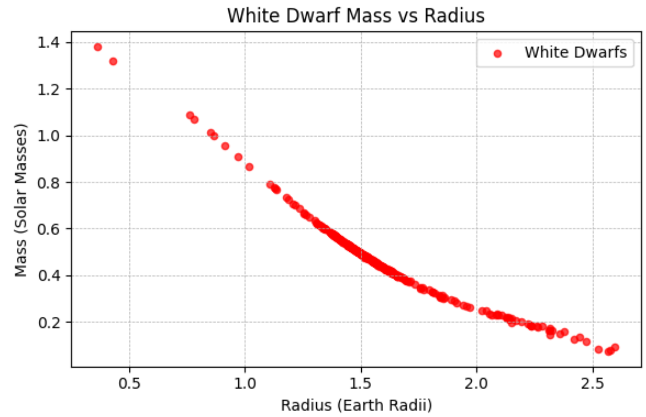

Figure 1: Mass vs. Radius of White Dwarfs on Linear Scale. Each point represents a white dwarf with its mass in solar masses and radius in Earth radii.

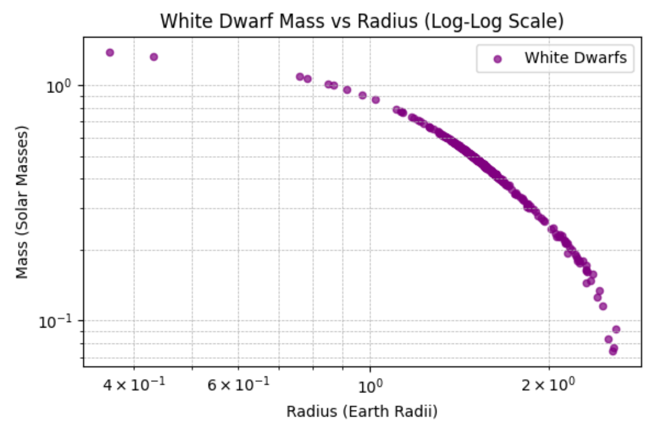

Figure 2: Mass vs. Radius of White Dwarfs on Log-Log Scale. This plot helps in identifying potential power-law relationships between mass and radius.

The scatter plots reveal an inverse relationship between mass and radius for white dwarfs, consistent with theoretical predictions from the theory of electron degeneracy pressure. As mass increases, the radius decreases, reflecting the balance between gravitational collapse and degeneracy pressure. The log-log plot further emphasizes this inverse relationship, suggesting a power-law dependence.

Part C: Analysis of the Mass-Radius Relationship in Low-Mass White Dwarfs

White dwarfs (WDs) are the final evolutionary endpoints of low- to intermediate-mass stars. Because of the extreme densities in their interiors, their structure is governed by electron degeneracy pressure. In this report, we focus on a subset of *low-mass* white dwarfs (typically $M \lesssim 0.4\,M_\odot$), for which certain simplifications in the equations of state (EOS) can be used.

Low-Mass Approximation

In low-mass white dwarfs, a particular limit of the equation-of-state expansion is valid. One can write

$$P = K^* \rho^{1+\frac{1}{n^*}},$$

where $n^* = \frac{q}{5-q}$ is the effective polytropic index in that limit, and q is typically an integer.

Power-Law Fits

First attempt a generic power-law fit:

$$M = A\, R^{\frac{3-n}{1-n}}$$

using a nonlinear least-squares procedure (e.g. `curve_fit` from `scipy`) as seen in 3. Following theoretical arguments, we set $q = 3$, leading to $n^* = 1.5$.

We refit with $n = 1.5$ fixed, obtaining a refined A^* as 1.91. Then, from 18 K^* is calculated as:

$$K^* = A\, 2859370.92$$

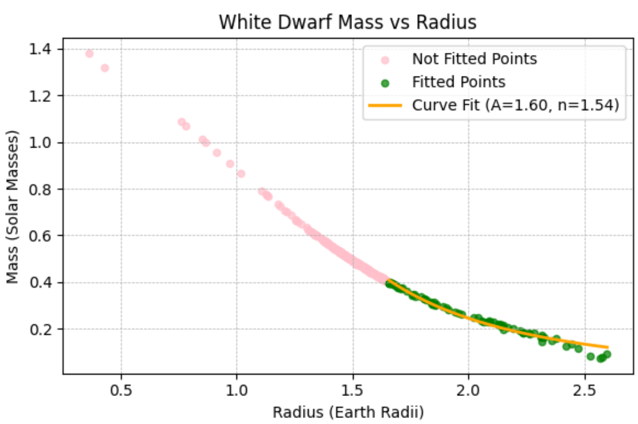

Figure 3: Mass vs. Radius curve-fit for $M \lesssim 0.4\, M_\odot$

Lane-Emden Solution

Next, the Lane-Emden equation for $n^* = 1.5$ to find the ξ_n and $\theta'(\xi_n)$ is solved as:

$$\xi_n = 3.65$$

$$\theta'(\xi_n) = -0.19$$

Central Density

Then a placeholder is produced estimate of the central density. Figure 4shows the central density vs. mass in linear space. The array of ρ_c values is uniform, since the code simply replicates a single ρ_c value for all data points in this demonstration.

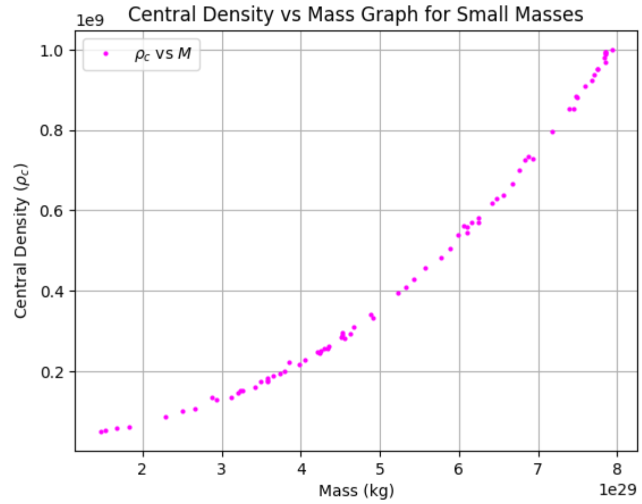

Figure 4: Mass (kg) vs. Central Density of White Dwarfs on Linear Scale.

A more rigorous analysis would do a full star-by-star calculation of ρ_c from the dimensionful Lane-Emden solutions, incorporating constants C, D, and physically appropriate boundary conditions.

Part D: General EOS and Interpolation Scheme

Now consider the full EOS (Eq. 8):

$$P = C\Big[x(2x^2 - 3)\sqrt{x^2+1} + 3\,\sinh^{-1}(x)\Big], \quad x = \left(\frac{\rho}{D}\right)^{1/q}.$$

Here, we have a 3-parameter family (C, D, q) if we treat q as known. If we have already found q from a low-mass fit, we can reduce the problem to 2 parameters (C, D).

However, to compute the mass-radius curve, we must solve the *full hydrostatic equilibrium* for each choice of (C, D, q), because $\rho(r)$ and $P(r)$ are related by this more complicated EOS. The star ends at the radius R where $\rho(R) = 0$.

The recommended approach:

- Pick a trial central density ρ_c.
- Numerically integrate from the center $r = 0$ outward until ρ goes to zero, giving $R(\rho_c)$ and $M(\rho_c)$.
- This yields a single point (M, R) for a chosen (C, D, q, ρ_c).
- By varying ρ_c, we trace out the entire $M(R)$ curve.

To fit the real data $\{(M_i, R_i)\}$, a multi-parameter search over (C, D, q) can be performed, or alternatively, q can be fixed while searching for (C, D). For each trial of (C, D), several ρ_c values are sampled, the integration is carried out, $M(R)$ is interpolated as seen in figure 5, and the error is computed against the real data. The (C, D) values that minimize the total error are calculated as:

$$D = (2.7 \pm 0.00001) \times 10^9$$

$$C = 9.36 \times 10^{21}$$

where theoretical values of these constants are:

$$D_{th} = 1.95 \times 10^{9}$$

$$C_{th} = 6.00 \times 10^{21}$$

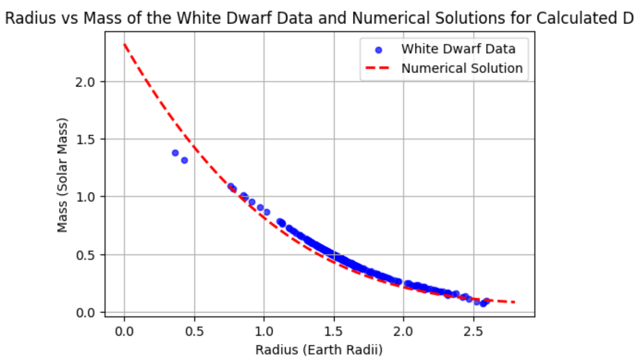

Figure 5: Mass vs Radius Numeric Solution for Calculated D

Part E: Chandrasekhar Limit and $n = 3$ Polytrope

In the ultra-relativistic limit, the EOS of a white dwarf tends to an $n = 3$ polytrope,

$$P \propto \rho^{4/3}.$$

Solving the Lane-Emden equation for $n = 3$ yields a dimensionless mass integral that is finite, hence leading to a maximum mass known as the Chandrasekhar mass:

$$M_{\text{Ch}} = \text{constant} \times \left(\frac{1}{\mu_e^2}\right),$$

where μ_e is the number of nucleons per electron (which depends on composition). Numerically,

$$M_{\text{Ch}} \approx 1.4\, M_{\odot}.$$

Empirically, once a C-O white dwarf surpasses this mass, electron degeneracy pressure can no longer support the star against gravitational collapse, leading to phenomena such as Type Ia supernova explosions.

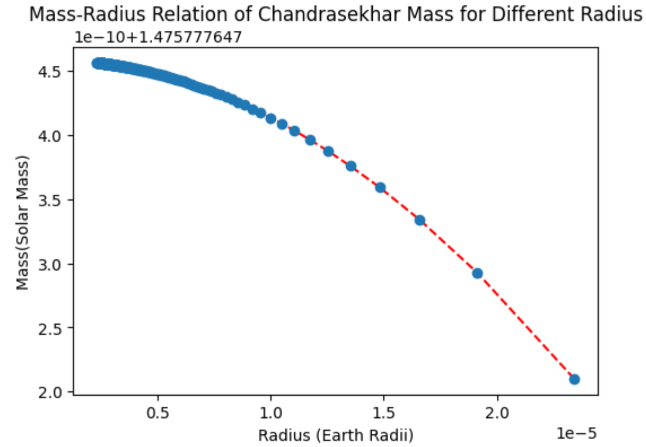

Figure 6: Mass Radius Relation of Chandrasekhar Mass for different Radius

Einstein

Neutron stars (NSs) are formed when the core of a massive star collapses under its own gravity during a supernova event. In these extreme objects, the gravitational force is balanced mainly by neutron degeneracy pressure (and nuclear interactions). At very high densities and pressures, general relativity (GR) must be used instead of Newtonian physics. Therefore, the Tolman-Oppenheimer-Volkoff (TOV) equation is employed to describe hydrostatic equilibrium in GR.

Newtonian hydrostatic equilibrium is usually given by the well-known balance:

$$\frac{dP}{dr} = -\rho \frac{GM(r)}{r^2},$$

where P is the pressure, ρ is the density, G is the gravitational constant, and $M(r)$ is the enclosed mass at radius r. In GR, this must be modified to the TOV form:

$$\frac{dP}{dr} = -\frac{G\left(\rho c^2 + P\right)\left(M(r)c^2 + 4\pi r^3 P\right)}{r\left(r - 2GM(r)/c^2\right)c^2}. \tag{1}$$

For convenience, geometric units ($c = G = 1$) are often adopted, simplifying the TOV equation to:

$$\frac{dP}{dr} = -\frac{(\rho + P)(M(r) + 4\pi r^3 P)}{r\left(r - 2M(r)\right)}, \tag{2}$$

with similar simplifications for ρ and $M(r)$.

In the polytropic model used here, the equation of state (EOS) is given by:

$$P = K_{\text{NS}}\rho^2, \tag{3}$$

where K_{NS} is the polytropic constant and ρ is the mass density.

Part A: Mass-Radius Relation

The TOV system can be written in first-order form by introducing variables for mass, metric potential, and pressure as functions of radius. The set of differential equations in geometric units often has the schematic form:

$$\frac{dm}{dr} = 4\pi r^2 \rho, \tag{4}$$

$$\frac{d\nu}{dr} = 2\,\frac{m + 4\pi r^3 P}{r(r-2m)}, \tag{5}$$

$$\frac{dP}{dr} = -\frac{1}{2}\,(\rho + P)\,\frac{d\nu}{dr}, \tag{6}$$

where ν is related to the metric coefficient, and $m(r)$ is the enclosed mass. An additional equation for the baryonic mass can also be introduced:

$$\frac{dm_p}{dr} = 4\pi \left(1 - \frac{2m}{r}\right)^{-\frac{1}{2}} r^2 \rho. \tag{7}$$

Figure 7 presents the neutron star mass as a function of radius for a fixed polytropic constant ($K_{\rm NS} = 100$). The code integrates from the center, where the pressure is specified by P_c, outward until the pressure drops below a specified threshold. The mass and radius are then extracted from the solution.

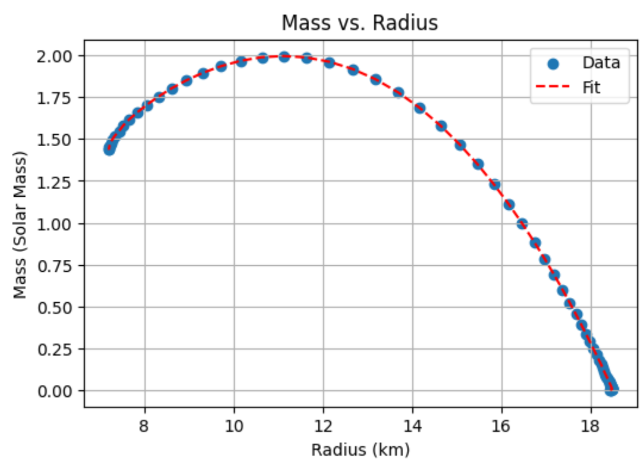

Figure 7: Mass vs. Radius curve for a chosen range of central pressures

It is observed that the mass increases rapidly with increasing radius until reaching a peak (the maximum mass) and then decreases with further increases in radius. This behavior is consistent with neutron star models: there is a maximum stable configuration beyond which the star is unstable or collapses to a black hole.

Part B: Fractional Binding Energy

The fractional binding energy Δ is defined as:

$$\Delta \equiv \frac{M_p - M}{M}, \tag{8}$$

where M is the gravitational mass (the mass that appears in the TOV solution) and M_p is the so-called "baryonic mass". Figure 8 shows the result of computing Δ as a function of radius.

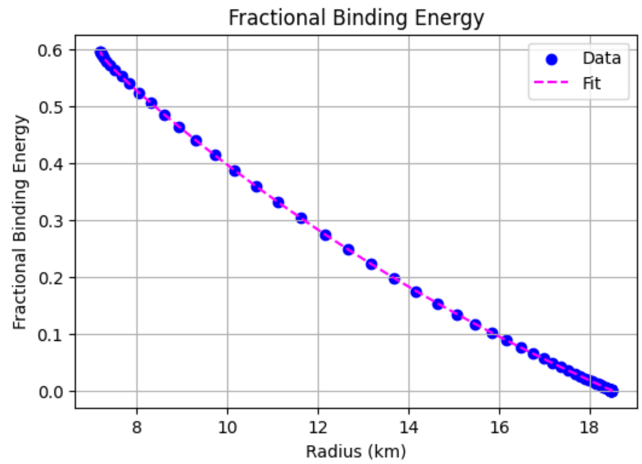

Figure 8: Fractional binding energy as a function of radius.

It can be seen that stars with smaller radii (higher central pressure/density) exhibit larger binding energy. As the radius grows and the star becomes less dense, the binding energy tends to zero.

Part C: Central Density vs. Mass and Stable and Unstable Branches

By varying the central density, different solutions for the mass and radius are obtained. In Figure 9, the mass is plotted as a function of the central density. The maximum of this curve indicates the maximum stable mass for the chosen polytropic constant.

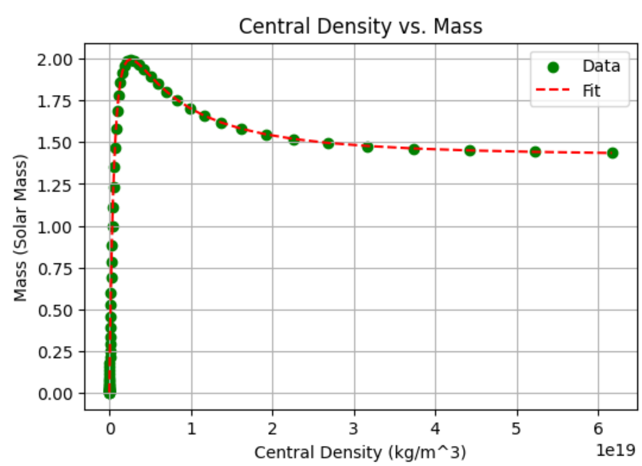

Figure 9: Mass vs. central density. The peak indicates the maximum mass configuration for the chosen EOS.

A commonly used criterion for stability in neutron stars is based on the slope $\frac{dM}{d\rho_c}$. Stars on the branch with positive slope (as mass increases with central density) are stable, while negative slope indicates instability:

$$\frac{dM}{d\rho_c} > 0 \quad \rightarrow \quad \text{stable,} \tag{9}$$

$$\frac{dM}{d\rho_c} < 0 \quad \rightarrow \quad \text{unstable.} \tag{10}$$

Figure 10 demonstrates how the mass-radius curve can be split into stable and unstable regions.

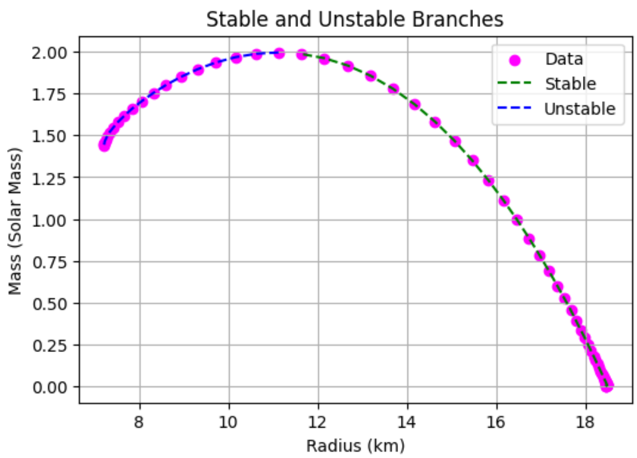

Figure 10: Mass vs. radius showing stable (green) and unstable (blue) branches.

Part D: Maximum Neutron Star Mass and Variation with K_{NS}K_NS

Finally, the maximum neutron star mass depends on the polytropic constant K_{NS}. Multiple solutions were generated by varying K_{NS}. The maximum mass found for each K_{NS} was determined.

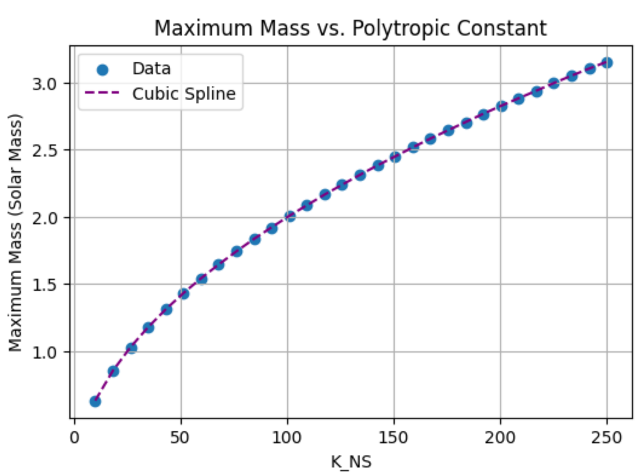

Figure 11: Maximum neutron star mass vs. polytropic constant K_{NS}.

By fitting these points with a spline, one can solve for the value of K_{NS} that gives a particular observed maximum mass. A result such as $K_{\mathrm{NS}} \approx 115.15$ might emerge from the numerical approach, indicating that higher values of K_{NS} allow higher maximum masses.

Part E

Since there is no matter outside the star, the pressure and mass can be generalized as $p(r > R) = 0$ and $m(r > R) = M$. The remaining equation for $\nu(r)$ simplifies to:

$$\nu'(r) = \frac{2M}{r(r - 2M)} \quad (r > R).$$

$$\nu(r) = C + \ln\left(1 - \frac{2M}{r}\right) \tag{11}$$

Where C is the constant to be determined from the initial value, which is $\nu(R)$. By evaluating the function at $r = R$, the expression for C is given as:

$$C = \nu(R) - \ln\left(1 - \frac{2M}{R}\right)$$

If we substitute this expression into the generic solution given in 11, we obtain the final expression for $\nu(r)$ for $r > R$:

$$\nu(r > R) = \ln\left(1 - \frac{2M}{r}\right) - \ln\left(1 - \frac{2M}{R}\right) + \nu(R)$$

Conclusion

This report presented a detailed investigation into the structure of stars, from Newtonian models to relativistic frameworks. The Lane–Emden equation provided insights into the mass-radius relationships of stars and white dwarfs, supported by observational data from the Montreal White Dwarf Database. These findings emphasize the utility of polytropic models in stellar astrophysics.

For neutron stars, the Tolman-Oppenheimer-Volkoff (TOV) equation was employed to account for general relativistic effects. The numerical solutions revealed key physical properties, such as the maximum mass, stable and unstable branches, and fractional binding energy. The dependency of maximum mass on the polytropic constant highlights the sensitivity of neutron star models to the chosen EOS.

Overall, this study underscores the critical role of both Newtonian and relativistic equations in understanding stellar evolution and compact objects. Future research could extend these models to include more complex EOS, rotation effects, or magnetic fields, further refining our understanding of the universe's most fascinating objects.

APPENDIX